Research article

The effects of transboundary air pollution from China on ambient air quality in South Korea

Moon Joon Kim [1,*]

Duke Kunshan University, China

A R T I C L E   I N F O

A B S T R A C T

This paper estimates the effects of wind direction on ambient air quality in South Korea (c.2006–2014) to provide insights into the impacts of the long-range transport of air pollutants from China. I find that the effect of transboundary air pollutants from China accounts for 19 percent of the weekly average PM_{10} concentrations, varying 12–30 percent by season. More specifically, winds blowing in the southwest direction have the largest year-round impacts on South Korea's ambient air pollution levels, which is consistent with the direction of emissions from Shanghai resulting in worse South Korean pollution levels. Further, the effects are differentiated seasonally according to the diverse activities that lead to the pollutants. Agricultural strawberry burning and coal-fired heating in northern Chinese cities lead to larger northwest wind effects in summer and winter, respectively. The winds from Shanghai have greater effects in spring due to the influence of dust storms passing from the deserts through mainland China.

1. Introduction

South Korea has experienced high levels of air pollution in recent years. According to research by the National Aeronautics and Space Administration (NASA, 2015) which observed air pollution trends worldwide over the last decade (2005–2014), Seoul is among the world's cities with the worst air pollution. Between 2009 and 2013, Seoul's mean PM_{10}[2] levels were higher than in many of the largest cities in the world: Los Angeles, Tokyo, Paris, and London (Korean National Institute of Environmental Research, 2015). Leem at al. (2015) estimate that air quality accounts for approximately 16 percent of total mortality in the Seoul metropolitan area in 2010.

To improve ambient air quality in the Seoul capital region, the South Korean government enacted the Special Act on Seoul Metropolitan Air Quality Improvement in December of 2003. The first metropolitan air pollution management plan was implemented in 2005 for a 10-year period (2005–2014). The metropolitan area includes Seoul and Incheon (cities) and Gyeonggi-do (a province). The pollutants considered for priority control were PM_{10}, nitrogen oxides (NO_X), sulfur oxides (SO_2), and volatile organic compounds (VOC_S). More specifically, the plan aimed to reduce average annual PM_{10} and NO_2 concentrations from 69 μg per cubic meter ($μg/m^3$) and 38 parts per billion (ppb) to 40 μg/m³ and 22 ppb by 2014, respectively.

Additionally, the Korean Ministry of Environment (2013) announced that long-range transboundary air pollution contributes approximately 30–50 percent of the total level of fine particles ($PM_{2.5}$)[3] in the air. The PM_{10} concentrations in Baekryeong-do, a South Korean island located close to Mainland China, increased by 44.5 percent when the wind was from the west (N) or northwest (NW). Li et al. (2014) and Park and Han (2014) estimate that the long-range transport of air pollutants from China accounts for approximately 26–30 percent of annual PM_{10} in South Korea, respectively. These studies, however, focus on the short-term event studies and do not consider the long-run average effects of transboundary pollutants.

China's air quality has declined and is expected to worsen because of the nation's dependence on coal to fulfill increasing energy demand.

Because prevailing winds in the region move from west to east and because South Korea is located east of China, air pollutants generated in Chinese industrial areas are transported to South Korea. South Korea has experienced sandstorms originating from deserts in west China and Inner Mongolia every spring for over 2,000 years. In recent years, the annual sandstorms have combined with other air pollutants, leading to serious damage.

The Chinese government has acknowledged that some emissions generated on their mainland may travel long distances and affect air quality in neighboring countries. In the 17th Tripartite Environment Ministers Meeting in Shanghai in April 2015, the environment ministers of South Korea, Japan, and China agreed to cooperate to improve forecasting accuracy for Asian dust storms, reduce air pollutant emissions, and share information to monitor and control pollutants. However, the level of attribution remains a subject of considerable debate.

This paper examines wind direction as a factor determining air pollutant levels in South Korea. The hypothesis is that air pollution and dust are likely to be generated in China due to coal-fired power generation and the naturally occurring Asian dust storms; therefore, pollution levels in South Korea will increase by westerlies. Evidence supporting this hypothesis suggests that China is a significant source of pollution problems in South Korea, and the quantitative magnitude of this increase would have important policy implications because of ongoing discussions between China and South Korea.

To conduct the analysis, two sets of data for air pollution concentrations and weather are combined. The data cover a nine-year period from 2006 to 2014 for seven metropolitan cities and nine provinces in South Korea. Daily mean PM_{10} concentrations were obtained from the Korea Environment Corporation (KECO). Weather data include precipitation, temperature, wind speed, and wind direction, and are publicly accessible through the Korea Meteorological Administrations (KMA).

I begin by focusing on the effects of westerly winds on PM_{10} concentrations and analyzing seasonal variations[4]. First, 16 wind directional dummy variables are generated to provide quantitative evidence of the relationship between daily air pollution levels and prevailing wind direction. Next, a westerly wind dummy is created; this dummy equals one if the azimuth wind direction is between 181 and 360° out of the west, and 0 otherwise[5]. The westerly wind dummy is included in the model to account for the marginal effect of westerlies on ambient air quality in South Korea, compared with an easterly wind. Splitting the west winds into seven bins with respect to azimuth angles, the contributions of each west wind (north-northwest, northwest, west-northwest, west, west-southwest, southwest, south-southwest) can then be calculated. In the regression models, both time- and city-fixed effects are included to control for unobserved heterogeneity that may affect air pollution levels.

I find that westerly wind increases PM_{10} concentrations in South Korea. The annual average effect of westerly wind on ambient PM_{10} is 19 percent, indicating that ambient PM_{10} levels increase by 9.5 μg/m^3 when the prevailing wind is out of the west based on annual average PM_{10} concentration (50 μg/m^3). The average effect is greatest in summer (30 percent), approximately one and a half times that of the annual average effect, and second largest in winter (21 percent). Thus, I conclude that various seasonal activities in China are likely to impact local PM_{10} concentrations in South Korea. These findings contrast with the South Korean government's claims and other studies where the Chinese contribution to PM_{10} in South Korea is 26–44.5 percent.

The major contribution of this study is the measurement of quantitative impacts of Beijing and Shanghai on ambient pollution levels in South Korea. The year-round effects of the winds from southwest directions (W, WSW, SW) are greater than the winds from northwest directions (NNW, NW, WNW). This finding suggests that areas near Shanghai emit more air pollutants that affect South Korean ambient air quality than areas around Beijing.

In winter, however, the ambient temperature in northern China is lower than in southern China, and a greater amount of fossil fuels are burned for heating. This results in poorer air quality in cities in the north of China compared with the cities in the south (Almond et al., 2009). Agricultural strawberry burning in northern China is a major factor causing high particulate matter levels in summer (Liu et al., 2018). Hence, the winds from the west or northwest have larger effects on South Korean air quality in summer and winter. In spring, west-southwest wind has greater effects than west-northwest wind. This finding indicates that dust from the deserts in southern China has a greater impact on South Korean PM_{10} concentrations than dust from Inner Mongolia.

2. Background

2.1. Asian dust storm

Every spring, huge dust storms hit countries in East Asia, such as China, South Korea, and Japan. The dust is generated from the dry desert regions in western China and Inner Mongolia where annual precipitation is less than 300 mm (Chang and Lee, 2007; In and Park, 2002; Mori et al., 2003; Hong et al., 2010). In South Korea, this yellow dust is said to be from Asian dust storms (ADSs), or yellow sand storms, or Kosa in Japan. ADS was first recorded over 2,000 years in both South Korea and China (Zhang, 1984; Chang and Lee, 2007; Lee, 2003). The storms blow over to the countries on the westerly wind and sometimes reach the western coast of North America (Husar et al., 2001; Chun et al., 2001; Uno et al., 2001).

An ADS can obstruct visibility and damage electronic goods, such as cars and factory machines, and cause pinkeye and respiratory and cardiovascular diseases. In South Korea, the mortality rate increased by 1.7 percent on ADS days in 1995–1998; the death rate from respiratory and cardiovascular problems increased by 4.1 percent (Kwon et al., 2002). The damages due to the storms in March 2002 were estimated at approximately USD$15.5 billion (Korean Government, 2008).

2.2. Prevailing westerlies

The westerlies are year-round prevailing winds from the west toward the east in the middle latitudes between 30 and 60°, and the Korean peninsula lies in the prevailing westerlies zone between 43° north and 33° north. In spring, dry sands from the deserts in China and Inner Mongolia travel long distances with these prevailing westerlies and become a sandstorm.

Figure 1 displays a wind rose based on daily wind direction and speed monitored in South Korea between Jan 1, 2006, to Dec 31,2014[6]. Because South Korea is located in the westerly zone, the west (W), west-northwest (WNW), northwest (NW) and north-northwest (NNW) winds account for more than 60 percent of the total wind direction. The winds from south-southeast (SSE), southeast (SE), and east-southeast (ESE) are less than 10 percent in total.

---

[4] Westerly winds are prevailing winds from the west toward the east in the middle latitudes between 30 and 60.

[5] Azimuth is defined as the angle formed between a reference direction, which is north of the reference plane, and a vector from the observer to a point of interest projected on the same reference plane as the reference direction orthogonal to the zenith, usually measured clockwise from the north point through 360°.

[6] A wind rose provides a succinct view of how wind speed and direction are typically distributed at a particular location. Presented in a circular format, the wind rose shows the frequency of winds blowing from particular directions. The length of each "spoke" around the circle is related to the frequency of time that the wind blows from a particular direction, US Department of Agriculture (https://www.wcc.nrcs.usda.gov/climate/windrose.html).
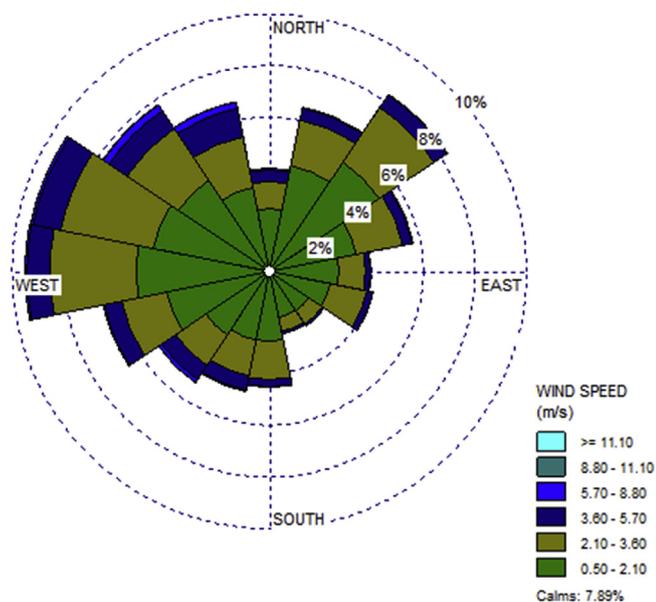
Figure 1. Wind rose between 2006 and 2014.
Notes: Wind rose is based on daily wind directions and speeds monitored in South Korea from 2006 to 2014.

2.3. Economic development and energy generation in China

China has developed rapidly in recent decades and its energy consumption has markedly increased simultaneously. Of the total, 87 percent of energy used depends on fossil fuels. Coal, the most carbon-intensive fuel, accounted for 70 percent of the total energy used in 2014. More than 4 billion tons of coal is burned in all sectors every year in China; less than 1 billion tons are burned in the United States, and 600 million tons are burned in Europe (Larson, 2014). China, therefore, accounted for 25 percent of global CO_2 emissions in 2011 and 80 percent of the worlds increase in CO_2 emissions since 2008 (Liu et al., 2013; Peters et al., 2012).

Of particular importance in this regard is that the locations of the polluting sources are concentrated in eastern China, which is sufficiently close to affect air quality in South Korea. For example, the distance between Beijing, the capital city of China, and Seoul, the capital city of South Korea, is 592 miles, and the distance between Shanghai and Seoul is 538 miles (approximately 866 km). Jeju-do (province), the southern island of South Korea, is 334 miles (approximately 538 km) from Shanghai. Figure 2 shows the geographical locations of interest in this study. Panel (a) displays Chinese coastal cities and provinces close to South Korea, including Beijing, Tianjin, Hebei, Jilin, Shanghai, Jiangsu, Zhejiang, and Shandong (in alphabetical order). Panel (b) shows the map of cities and provinces in South Korea, including Busan, Chungbuk, Chungnam, Daegu, Daejeon, Gangwon, Gwangju, Gyeongbuk, Gyeonggi, Gyeongnam, Incheon, Jeju, Jeonbuk, Jeonnam, Sejong, Seoul, and Ulsan (in alphabetical order). Sejong was a new city separated from Chungnam in 2010 and is included in Chungnam in this study for simplicity.

2.4. Wind and air quality

South Korea is under the pathway of westerlies, and meteorological conditions play a role in the transport of air pollution. Guo et al. (2014) compare different mass concentrations according to the wind directions during clean and polluted seasons and find that a relationship between wind patterns and particle concentrations exists. The authors indicate that meteorological conditions regulate the periodic cycle of PM events in Beijing and assert that the regional transport of particles is one of the key factors. The prevailing winds on clear days are the winds from unpolluted areas, and the prevailing winds during polluted periods are the winds from polluted industrial areas. The wind speeds from industrial areas are lower than those from clean regions because of the heavily polluted air masses. Streets et al. (2007) also show that fine particles ($PM_{2.5}$) from Hebei traveling on prevailing wind from north to south account for approximately 32 percent of monthly average $PM_{2.5}$ concentrations in Beijing.

3. Data

This paper uses two sets of data: daily average concentrations of air pollutants and daily weather monitoring data in South Korea, see Supplementary Material. Both daily data sets cover nine years (2006–2014) for seven metropolitan cities (Seoul, Busan, Incheon, Daegu, Daejeon, Gwangju, Ulsan) and nine provinces (Gyeonggi-do, Gangwon-do,

(a) Chinese coastal provinces

(b) South Korean provinces
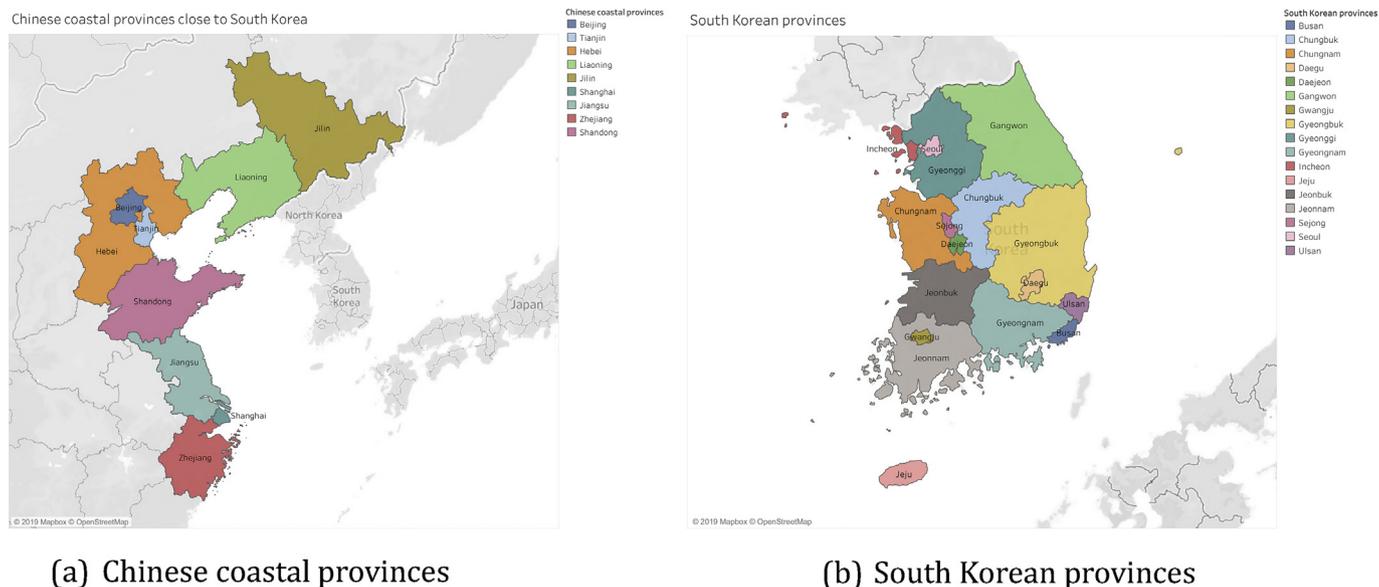
Figure 2. Chinese coastal provinces and South Korean provinces.*Notes*: Chinses coastal cities and provinces include Beijing, Tianjin, Hebei, Liaoning, Jilin, Shanghai, Jiangsu, Zhejiang, and Shandong. South Korea cities and provinces include Busan, Chungbuk, Chungnam, Daegu, Daejeon, Gangwon, Gwangju, Gyeongbuk, Gyeonggi, Gyeongnam, Incheon, Jeju, Jeonbuk, Jeonnam, Sejong, Seoul, and Ulsan. All cities and provinces are listed in alphabetical order. Sejong was a new city separated from Chungnam in 2010 and is included in Chungnam in this study for simplicity.

Gyeongbuk-do, Gyeongnam-do, Jeonbukdo, Jeonnam-do, Jeju-do, Chungbuk-do, and Chungnam-do).

3.1. Air pollution data

The daily average PM_{10} concentrations data are obtained from KECO. Real-time data is collected from each monitoring station using the electrochemical method and reported to the National Ambient Air Monitoring Information System (NAMIS). NAMIS aggregates the data (approximately 3.4 hundred million observations per year) from 317 monitors: city (257), suburb (19), roadside (38), national ambient (3), and air quality measurement in 97 cities and counties (as of 2014). The air pollution concentrations data have been publicly released since December 28, 2006.

City-level daily mean PM_{10} ambient concentration is calculated as an average monitor within a city:

$$\overline{PM10_{cd}} = \frac{1}{M} \sum_{m=1}^{M_c} \overline{PM10_{cdm}} \tag{1}$$

where

$\overline{PM10_{cd}}$ = mean ambient concentration in city (c), on day (d)
$\overline{PM10_{cdm}}$ = mean ambient concentration at monitor (m) in city (c) on day (d)
M_c = number of monitoring stations in city (c)

3.2. Meteorological data

The weather data are available from the National Climate Data Service System website, managed by the KMA and comprise precipitation, temperature, wind speed, and wind direction. The weather monitoring stations are less numerous and more evenly geographically dispersed than the air quality monitoring stations, which are more concentrated according to population. The precipitation variable indicates the daily accumulated amount of precipitation. The temperature variable is an average daily value of eight 3-hour interval observations: at 3, 6, 9, 12, 15, 18, 21, and 24 o'clock during a day. The average wind speed is the daily mean speed of the total daily wind run[7]. The wind direction variable records the prevailing wind direction that occurs most frequently during eight 3-hour intervals at a certain monitoring station.

3.3. Summary statistics

Table 1 reports sample statistics for the key variables. The annual mean PM_{10} concentration is 49.59 μg/m³, which is approximately 2.5 times the World Health Organization Air Quality Guideline of 20 μg/m³ as the annual mean. The mean PM_{10} concentration is 62.26 μg/m³ in spring and 54.41 μg/m³ in winter, higher than the annual average. Because of the ADS, the mean and maximum levels of PM_{10} peak in the spring. However, mean PM_{10} in winter is the second highest, when the impact of the ADS is slight.

3.4. Data transformation

Because the two data sets are collected from different sources, a two-step data transformation is conducted for the study. First, the daily observed data from each monitoring station are aggregated spatially to the city or province level. Next, the day-by-city level data are aggregated temporally to the weekly level.

Table 1. Summary statistics.

Variable	Observation	Mean	Median	SD	Min	Max
PM10						
-year round	52534	49.59	44	31.25	2	992
-spring	13104	62.26	55	43.75	4	992
-summer	13100	37.72	34	17.68	2	147
-fall	13092	43.89	38	23	5	639
-winter	13238	54.41	48	28.20	4	507
Precipitation	52592	3.73	0	12.67	0	110
Temperature	52591	13.21	14.29	9.66	-14.56	33.10
Wind speed	52590	1.90	1.7	1.25	0.007	11.91

Notes: The panel data is balanced. Data include daily observations of PM10 and meteorological conditions during nine years (2006–2014) for seven metropolitan cities (Seoul, Busan, Incheon, Daegu, Daejeon, Gwangju, Ulsan) and nine provinces (Gyeonggi-do, Gangwon-do, Gyeongbuk-do, Gyeongnam-do, Jeonbukdo, Jeonnam-do, Jeju-do, Chungbuk-do, and Chungnam-do). Precipitation is measured in millimeter (mm) units. Temperature is measured in Celsius ($C°$) units. Wind speed is measured in meter per second (m/s) units.

3.4.1. Observatory level to city level

Since the data are collected by different organizations, there are some differences in the number and the location of the monitoring stations. The number of air pollution monitoring stations is dependent on the size of the city, and industrial cities have more monitors. Because of these differences in data collection, the mean values of weather and air pollution variables for each city and province are calculated and used in this study, except for wind direction and wind speed.

The average wind direction and speed cannot be calculated by a simple arithmetic calculation because performing a simply aggregate across degree measures of radial orientation is not possible. For example, the arithmetic mean of the two wind directions $1°$ and $359°$ is $180°$, but both directions are very close to North ($0°$) and, therefore, their average should be $0°$. In this paper, I calculate the mean wind direction and speed by the vector calculations used in the U.S. Environmental Protection Agency Meteorological Monitoring Guidance for Regulatory Modeling Applications[8]:

$$V_{ce} = -\frac{1}{N} \sum u_{ci} \sin(\theta_{ci}) \tag{2}$$

$$V_{cn} = -\frac{1}{N} \sum u_{ci} \cos(\theta_{ci}) \tag{3}$$

$$WS_{cd} = \left(V_{ce}^2 + V_{cn}^2\right)^{\frac{1}{2}} \tag{4}$$

$$WD_{cd} = \arctan\left(\frac{V_{ce}}{V_{cn}}\right) + FLOW \tag{5}$$

where

$$FLOW = \begin{cases} +180 \; for \; \arctan\left(\frac{V_{ce}}{V_{cn}}\right) < 180 \\ -180 \; for \; \arctan\left(\frac{V_{ce}}{V_{cn}}\right) > 180 \end{cases}$$

θ_{ci} = azimuth angle of the wind direction, measured clockwise from the north at monitor (i) in city (c)
u_{ci} = wind speed measured at monitor (i) in city (c)
V_{ce} = magnitude of the east-west component of the resultant vector mean wind
V_{cn} = magnitude of the north-south component of the resultant vector mean wind

---

[7] Wind run is a meteorological term used to categorize or determine the total distance of the traveled wind over a period of time.

[8] https://www3.epa.gov/scram001/metguidance.htm.

This approach is based on the vector mean calculation, where the wind direction is weighted by the wind speed. I first compute the wind speed-weighted East-West vector component (V_{ce}) and North-South vector component (V_{cn}) of each wind direction observation θ_i. In Eqs. (4) and (5), the two components V_{ce} and V_{cn} are converted into the city (province)-by-day level mean wind direction (WD_{cd}), and mean wind speed (WS_{cd}).

3.4.2. Daily to weekly

A priori the time scales for the transport of air pollution from China to South Korea are estimated to be approximately one to seven days. To minimize the effects of time variation in transport, the daily data are converted to weekly. The arithmetic mean is used for all variables except wind direction. The mean value of wind direction is defined in the following regression models.

The aggregated level of the data might generate lower estimates because of the large variance of air pollution levels. Figure 3 illustrates the box plots for PM_{10} for 16 cities and provinces. The box plots display the PM_{10} data broken into four quartiles. The plots show that many outliers exist. These outliers are critical because of the potentially higher contribution of China to extremely high PM_{10} levels in South Korea. Further research should consider those outliers to fully explain the wind-related effects of transboundary air pollution on ambient air quality.

4. Empirical strategy

In this section, I econometrically identify the role of wind in local air quality. The regression models used in the analysis identify the marginal effect of prevailing wind direction on air pollution and how it varies with source direction, allowing a determination of which directions of wind have the greatest impacts. The parameters of interest in the models are the coefficients of the wind direction dummies, which capture, for example, the marginal effect of the west wind, apart from the effect of the east wind.

4.1. Effects of westerly wind on PM_{10} concentrations

To estimate the effect of westerly wind on PM_{10} concentration in Korea, I first estimate:

$$PM10_{cw} = \alpha + \beta_1 Precip_{cw} + \beta_2 Temp_{cw} + \beta_3 WS_{cw} + \beta_4 1(Direct_{cw}) + \eta_w + \delta_c + \varepsilon_{cw}$$
(6)

where c and w reference a city/province and week, respectively. The dependent variable in this model is the log of the weekly average PM_{10} in a city and province. The precipitation (*Precip*), temperature (*Temp*), wind
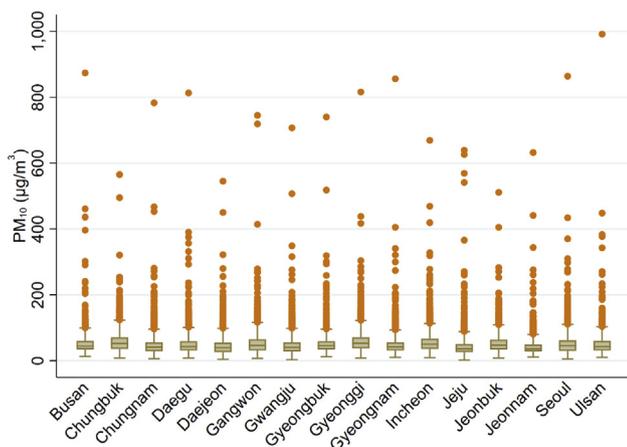
speed (*WS*) variables are included as control variables. The regression includes week-by-year fixed effects (η_w) and city fixed effects (δ_c), which control for time-varying shocks and underlying differences in air pollution levels based on geography.

The dummy for westerly wind, $1(Direct)$ equals 1 if the azimuth degree of the wind direction is between 181 and 360, and 0 otherwise. Rather than using the simple weekly aggregation of the dummy variable, ranging from 0 to 7, I construct a weekly-weighted indicator variable, which is a share of the number of days where the wind blows from a certain direction. Each daily prevailing wind direction is assigned a binary value, either 1/7 if the wind blows from the west or zero otherwise. For example, if a west wind is the prevailing wind for three days and east wind prevails for four days, the weekly weighted value for the westerly wind dummy is 3/7, assigning zero weight to winds other than westerlies. The coefficient of interest is β_4, which captures the effect of westerly wind on PM_{10} levels. This parameter assesses the extent to which westerly wind leads to higher PM_{10}, compared with easterly wind.

4.2. Effects of separate west winds on PM_{10} concentrations

Discretizing the compass, there are seven west winds (from the north and counterclockwise): north-northwest (NNW), northwest (NW), west-northwest (WNW), west (W), west-southwest (WSW), southwest (SW), and south-southwest (SSW). To find the most influential wind direction, each of the seven wind directions is used as the reference wind direction in a separate regression. Next, the daily prevailing wind direction is weighted by the truncated cosine function, which provides the highest weight ($= 1$) when the daily prevailing wind corresponds to each reference west wind direction, X, and the lowest weight ($= 0$) when the difference in angle between the daily prevailing wind and each reference direction is equal to or greater than $90°$. I repeat this regression seven times, once for each reference west wind direction:

$$PM10_{cw} = \alpha + \beta_1 Precip_{cw} + \beta_2 Temp_{cw} + \beta_3 WS_{cw} + \beta_4 Tcos(Direct_{cw} = X)$$
$$+ \eta_w + \delta_c + \varepsilon_{cw}$$
(7)

where X = NNW, NW, WNW, W, WSW, SW, SSW

Eq. (7) is a smoother transformation of Eq. (6). Rather than using a dummy variable, $1(Direct)$, Eq. (7) uses a cosine-shaped filter for the wind

Figure 3. Box plots for PM_{10} by city and province.
Notes: Box plots describe the quartiles of the data and outliers.
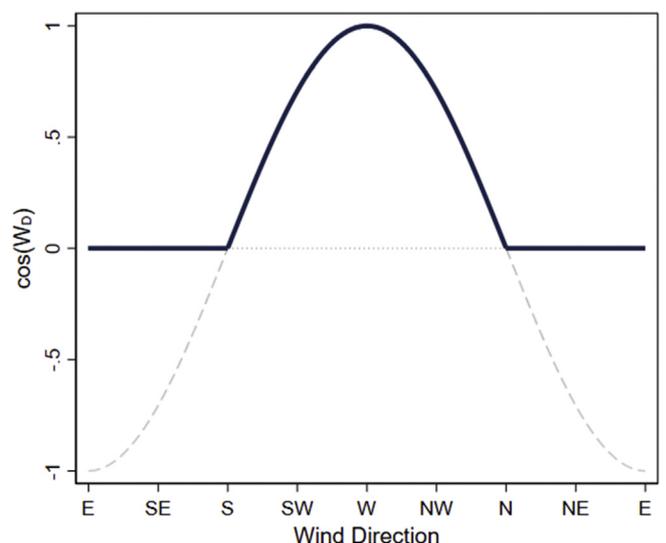

Figure 4. Example of truncated cos (west wind).
Notes: The truncated cosine function provides the highest weight ($= 1$) if the daily prevailing wind corresponds to the reference wind, the west wind in this example. The cosine value diminishes as the wind direction shifts farther away from the west and eventually becomes zero when the wind direction reaches south or north.
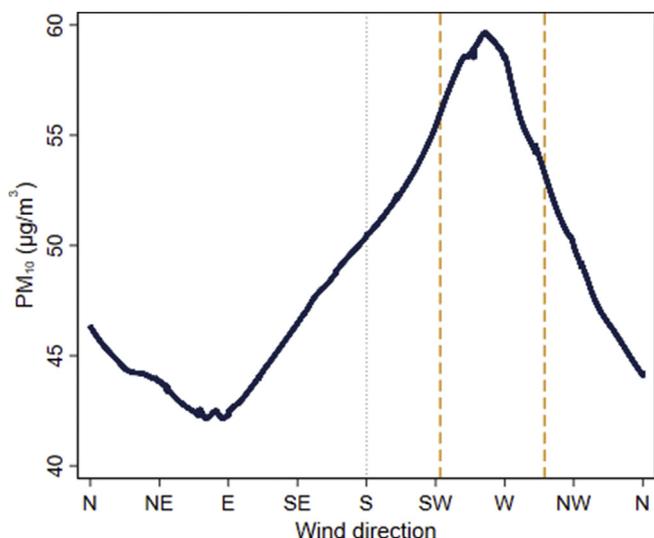
Figure 5. PM_{10} concentrations by wind directions (2006–2014).
Notes: Locally Weighted Scatterplot Smoothing (LOWESS) with a bandwidth of 0.2. The left dashed line indicates the mean direction from Shanghai toward South Korea. The right dashed line indicates the mean direction from Beijing toward South Korea.

Table 2. Marginal effects of the westerly wind on PM_{10} concentrations.

	Year round	Spring	Summer	Fall	Winter
Precipitation	-0.003*	-0.009***	-0.003***	-0.002	-0.001
	(0.001)	(0.002)	(0.001)	(0.002)	(0.001)
Temperature	0.001	0.003	0.010	0.002	-0.003*
	(0.002)	(0.002)	(0.007)	(0.001)	(0.001)
Wind speed	-0.031*	-0.030*	-0.007	-0.011	-0.028
	(0.016)	(0.016)	(0.018)	(0.032)	(0.019)
1 (Direct)	0.076***	0.084**	0.151***	0.052*	0.096**
	(0.020)	(0.034)	(0.037)	(0.027)	(0.033)
city-fixed effect	Yes	Yes	Yes	Yes	Yes
time-fixed effect	Yes	Yes	Yes	Yes	Yes
R2	0.861	0.848	0.805	0.856	0.837
Observation	7487	1872	1872	1872	1871

Notes: Robust standard errors are in parentheses and clustered at the city level to control for correlation within a cluster. Precipitation is measured in millimeter units. Temperature is measured in Celsius (C°) units. Wind speed is measured in meter per second (m/s) units. The estimate of the westerly wind shows that weekly PM_{10} increases by 7.9 percent if prevailing wind blows out of the west. The percentage change in PM10 by westerly winds is approximated as $(\exp(\beta_4 - 1)) \times 100$.

*** Significant at the 1 percent level.
** Significant at the 5 percent level.
* Significant at the 10 percent level.

direction variable. The variable *Tcos(Direct = X)* indicates a truncated cosine value of each wind direction, oriented with respect to the west. Figure 4 illustrates how this truncated version of the cosine function captures westerly effects to determine the effect of the wind from the west (by setting the west wind as a reference, X = W), the cosine function produces the value of one if the wind blows from the west (W). The cosine value diminishes as the wind direction gets farther away from the west and eventually becomes zero when the wind direction reaches south (S) or north (N). The trigonometric cosine function is truncated so that directions greater than $\pi/2$ radians (90˚) away from the west take a value of 0. An average of the seven daily truncated cosine values for each week is included in the regression.

The parameter of interest is the coefficient of *Tcos(Direct = X)*, β_4. For each regression, β_4 represents the estimate of the "reference-weighted" wind direction[9]. I compare the estimates of the seven β_4 and R^2 from each regression. The reference wind direction with the greatest β_4 implies the largest effects on PM_{10}, and R^2 suggests which specification fits the data best. In all regressions, the robust standard errors are clustered at the city/province level.

5. Results

Figure 5 is a graphical summary of the relationship between two variables: daily prevailing wind directions and the daily mean PM_{10} concentrations from 16 cities and provinces in South Korea in 2006–2014. The fitted curve is obtained from non-parametric regression using locally weighted scatterplot smoothing (LOWESS) with the tricube weight function and a bandwidth of 0.2 (Cleveland, 1979). The simplest means to smooth a scatterplot is to use a moving average (running mean). Using the running means may result in bias that gives less importance to the closest neighbors and more to those farther away. To prevent this bias, the running lines are used to smooth a scatterplot.

The graph shows that daily average PM_{10} concentrations decrease as the wind direction shifts to the east, reaching a minimum when the wind is from the east (E). Then, PM_{10} levels increase as more winds blow from the west and peak between the southwest and west. It starts to decrease again as the wind direction shifts to the north. The left dashed line

indicates the mean direction from Shanghai toward South Korea. The right dashed line presents the mean direction from Beijing toward South Korea. From this graph, I obtain a preview of two main results. First, there is a significant relationship between wind direction and local PM_{10} concentrations in South Korea. Second, pollutants generated from areas near Shanghai have larger impacts on PM_{10} levels in South Korea than the pollutants from areas near Beijing. The two endpoints on the left and right represent north, which is the same direction. The discrepancy between the two values is due to the air pollution effect of the wind direction, which should have been approximated in three dimensions, and was approximated in two dimensions through the LOWESS.

Table 2 reports results from Eq. (6). The estimates indicate the marginal effects of the westerly wind on the PM_{10} levels compared with the east winds. The first column covers the entire year, and the other columns are split into the four seasons to assess whether the average effects are temporally stable. I posit that the negative signs for the coefficients of precipitation and wind speed seem reasonable because of flushing effects.[10] One of the notable results is the negative sign of temperature in winter. This can be interpreted as an increase in pollutants emitted by energy generation for heating in China when the temperature decreases.

The estimate of the westerly winds is 0.076, implying that PM10 increases by 7.9 percent if the wind is out of the west[11]. This finding can be interpreted to mean that weekly westerly prevailing wind is associated with a 3.77 μg/m³ increase in weekly mean PM_{10} concentration. Seasonally, the estimate is the highest in summer (15.1 percent) and second highest in winter (9.6 percent). The results suggest that the effect of transboundary air pollution from China peaks in summer and winter when more pollutants are generated in China because of agricultural strawberry burning and heating, respectively.

Table 3 presents the results from Eq. (7). For comparison, Table 3 includes a summary of estimates from seven separate regressions and indicates each wind's marginal contribution to PM_{10} concentration

---

[9] The term, reference-weighted wind direction, means the weighted wind direction by the truncated cosine function, which gives the highest value to the wind direction that corresponds to each reference wind direction.

[10] Strong winds tend to lower the concentration of pollutants by spreading them apart as they move downstream This process of spreading is called *dispersion* or *flushing*.

[11] Since the dependent variable, PM10, is log-transformed, the percentage change in PM10 by westerly winds is approximated as $(\exp(\beta_4) - 1) \times 100$.

Table 3. Marginal effects of seven west winds (W) on PM_{10} concentrations.

	(1)	(2)	(3)	(4)	(5)	(6)	(7)
	NNW	NW	WNW	W	WSW	SW	SSW
(a) Year round	-0.054	0.034	0.100***	0.139***	0.164***	0.158***	0.122**
(N = 7487)	(0.061)	(0.046)	(0.028)	(0.031)	(0.038)	(0.048)	(0.057)
R2	0.859	0.859	0.861	0.863	0.864	0.863	0.861
(b) Spring	-0.034	0.042	0.085*	0.105**	0.127***	0.124***	0.099***
(N = 7487)	(0.036)	(0.038)	(0.041)	(0.040)	(0.033)	(0.029)	(0.030)
R2	0.847	0.847	0.848	0.849	0.849	0.849	0.848
(c) Summer	0.137**	0.207***	0.205***	0.203***	0.201***	0.148**	0.050
(N = 7487)	(0.051)	(0.053)	(0.049)	(0.048)	(0.052)	(0.055)	(0.047)
R2	0.800	0.804	0.806	0.806	0.805	0.801	0.797
(d) Fall	0.007	0.039	0.076*	0.102**	0.116***	0.106**	0.065
(N = 7487)	(0.051)	(0.047)	(0.038)	(0.036)	(0.037)	(0.037)	(0.044)
R2	0.855	0.855	0.856	0.857	0.858	0.857	0.856
(e) Winter	0.028	0.108**	0.135***	0.140***	0.129***	0.091***	0.037
(N = 7487)	(0.036)	(0.048)	(0.041)	(0.037)	(0.034)	(0.029)	(0.035)
R2	0.834	0.837	0.839	0.840	0.838	0.836	0.834

Notes: Robust standard errors are in parentheses and clustered at the city level to control for correlation within a cluster. Columns (1)–(7) are the results from the regressions using a truncated cosine function for each reference west wind direction (north-northwest, northwest, west-northwest, west, west-southwest, southwest, south-southwest). Rows (a)–(e) show the results from seasonal analysis (Spring: March, April, May; Summer: June, July, August; Fall: September, October, November; Winter: December, January, February). All regressions include city and time fixed effects as well as controls for precipitation, temperature, and wind speed.

  *** Significant at the 1 percent level.

  ** Significant at the 5 percent level.

  * Significant at the 10 percent level.

Table 4. Marginal effects of seven east winds (E) on PM_{10} concentrations.

	(1)	(2)	(3)	(4)	(5)	(6)	(7)
	NNE	NE	ENE	E	ESE	SE	SSE
(a) Year round	-0.133***	-0.140***	-0.128***	-0.120***	-0.091*	-0.051	-0.004
(N = 7487)	(0.041)	(0.033)	(0.029)	(0.033)	(0.044)	(0.049)	(0.049)
R2	0.862	0.862	0.861	0.861	0.860	0.859	0.859
(b) Spring	-0.119***	-0.151***	-0.156***	-0.138***	-0.075	-0.018	0.013
(N = 7487)	(0.038)	(0.037)	(0.035)	(0.043)	(0.049)	(0.044)	(0.036)
R2	0.849	0.850	0.850	0.849	0.847	0.847	0.847
(c) Summer	-0.078	-0.156**	-0.209***	-0.235***	-0.205***	-0.143**	-0.094**
(N = 7487)	(0.060)	(0.054)	(0.049)	(0.054)	(0.054)	(0.050)	(0.044)
R2	0.798	0.801	0.804	0.807	0.805	0.802	0.799
(d) Fall	-0.038	-0.053	-0.066	-0.088*	-0.107*	-0.122*	-0.087
(N = 7487)	(0.042)	(0.039)	(0.038)	(0.046)	(0.056)	(0.059)	(0.062)
R2	0.855	0.856	0.856	0.856	0.857	0.857	0.856
(e) Winter	-0.105***	-0.126***	-0.126***	-0.130***	-0.128***	-0.119**	-0.083
(N = 7487)	(0.035)	(0.040)	(0.041)	(0.041)	(0.038)	(0.050)	(0.057)
R2	0.837	0.838	0.838	0.837	0.836	0.836	0.835

Notes: Robust standard errors are in parentheses and clustered at the city level to control for correlation within a cluster. Columns (1)–(7) are the results from the regressions using a truncated cosine function for each reference west wind direction (north-northeast, northeast, east-northeast, east, east-southeast, southeast, south-southeast). Rows (a)–(e) show the results from seasonal analysis (Spring: March, April, May; Summer: June, July, August; Fall: September, October, November; Winter: December, January, February). All regressions include city and time fixed effects as well as controls for precipitation, temperature, and wind speed.

  *** Significant at the 1 percent level.

  ** Significant at the 5 percent level.

  * Significant at the 10 percent level.

compared with its opposite wind direction. I find that northwest wind (NW) and west-northwest wind (WNW), indicating winds from Beijing to South Korea, have the greatest effects in summer and winter. Furthermore, the west-southwest (WSW) wind and southwest (SW) wind show the strongest impacts in spring and fall; the wind corresponds to the direction from Shanghai to South Korea. These findings are meaningful because they not only suggest the effects of transboundary air pollutants from China but also provide information on the locations of their main sources.

Last, using the aforementioned results, I estimate the net effects of Chinese emissions on Korean PM_{10} levels. First, I examine the marginal effects of winds blowing out of all other directions and the estimates of the all other winds have negative marginal effects on PM_{10}, indicating that air pollution decreases as more winds from other directions blow. In Table 4, when wind blows from a clean, unpolluted area, flushing is effective in reducing air pollution because the air circulates through the wind.

Table 5. Net average effects of westerly winds on PM_{10}.

	Year round	Spring	Summer	Fall	Winter
Westerly winds (WEST)	9.97	9.11	16.72	6.93	11.04
All other winds (AO)	-8.68	-7.41	-12.89	-5.35	-9.51
Net effect (WEST-AO)	18.65	16.52	29.61	12.29	20.55

Notes: The average effects of westerly and all other winds are the product of the marginal effect and the observed share of each wind direction. The net effect of Chinese emissions is the difference between average effect of westerly winds and all other winds *(WEST-AO)*.

5.1. If Chinese emissions had no influence on South Korean pollution levels, westerlies

would also show the flushing effect. Considering the characteristics of winds, I estimate the net effects of winds blowing from China by using the difference between the average effects of the westerlies and all other winds. Eqs. (8) and (9) show how the average effects of westerly and all other winds are calculated:

$$WEST = \sum_{WD=SSW}^{NNW} \left[\Delta WD \times S_{WD}^{WEST} \right] \tag{8}$$

$$AO = \sum_{WD=S}^{N} \left[\Delta WD \times S_{WD}^{AO} \right] \tag{9}$$

$$Net\ effect = WEST - AO \tag{10}$$

where S_{WD} is the share of each wind direction among the winds from the west or all other winds. The marginal effects of seven different wind directions ($4WD$) are multiplied by the weight (S_{WD}), which is the observed share of wind from that direction over the nine-year period. The net effect, which is the difference between the two effects, is shown in Eq. (10).

Table 5 displays the net average effects of winds from China on Korean PM_{10} levels. The estimates in the first row display the average effects of particles on wind from China each season and the second row shows the flushing effects of wind blowing from the all other directions. The difference between these two effects is the net average effect of the winds from China on South Korean PM_{10}, shown in the third row. Nineteen percent of the weekly average PM_{10} concentration in South Korea is due to China's emissions. This amount accounts for 21 percent in winter when electricity is used for heating, and 17 percent in spring although the effect of ADS is considered. The net effect is the largest in summer due to agricultural strawberry burning, 30 percent, but it has not been recognized as a serious problem because of the high temperature, which easily disperses air pollutants, and the concentration of precipitation in summer.

6. Conclusion

In the last decade, the levels of air pollution in South Korea have increased. Along with local polluting sources, the long-range transport of air pollutants has become a critical environmental and economic problem. In 2013, a study commissioned by the South Korean government claimed that transboundary air pollution from China contributed 30–50 percent of the total level of fine particles ($PM_{2.5}$) in South Korea. These effects are expected to increase as the generating capacity of coal-fired power plants increases in China (Larson, 2014).

This paper estimates the effects of long-range transport of air pollution from China on ambient air quality in South Korea. This aim is accomplished through a novel empirical specification that uses wind direction to predict the likely impacts of naturally occurring and man-made emissions from China on South Korean ambient pollution levels.

I find that winds blowing from China to South Korea have significant impacts on South Korean local PM_{10} concentrations.

More specifically, southwest winds have the largest year-round impact, indicating that more of the air pollutants that affect South Korean ambient air quality are from Shanghai, rather than Beijing. Seasonally, the northwest winds have the largest effects on South Korean PM_{10} levels in summer and winter because of agricultural strawberry burning and coal-fired heating in northern Chinese cities. The ADSs passing through mainland China result in the southwest winds having the greatest effects on the South Korean PM_{10} concentrations in spring.

One limitation of the analysis in this paper is notable. Due to limitations in the data source, this study uses the data aggregated to daily measurement intervals, which averages out extreme values during a day. This aggregated level data can, therefore, lead the estimates for the effect of wind to be underestimated. For a more precise estimate, further analysis with hourly data that includes extreme observations during 24-hour periods could be conducted.

Declarations

Author contribution statement

Moon Joon Kim: Conceived and designed the experiments; Performed the experiments; Analyzed and interpreted the data; Contributed reagents, materials, analysis tools or data; Wrote the paper.

Competing interest statement

The authors declare no conflict of interest.

Additional information

Supplementary content related to this article has been published online at https://doi.org/10.1016/j.heliyon.2019.e02953.

References

Almond, D., Chen, Y., Greenstone, M., Li, H., 2009. Winter Heating or Clean Air? Unintended Impacts of China's Huai River Policy. Am. Econ. Rev. 99 (2), 184–190.

Chang, S.C., Lee, C.T., 2007. Assessment of PM10 enhancement by yellow sand on the air quality of Taipei, Taiwan in 2001. Environ. Monit. Assess. 132 (1–3), 297–309.

Cleveland, W., 1979. Robust Locally Weighted Regression and Smoothing Scatterplots. J. Am. Stat. Assoc. 74 (368), 829–836.

Chun, Y., Boo, K., Kim, J., Park, S., Lee, M., 2001. Synopsis, transport, and physical characteristics of Asian dust in Korea. J. Geophys. Res. 106 (D16), 18,461–18,469.

Guo, S., Hu, M., Zamora, M., Peng, J., Shang, D., Zheng, J., Du, Z., Wu, Z., Shao, M., Zeng, L., Molina, M., Zhang, R., 2014. Elucidating severe urban haze formation in China. P. Natl. Acad. Sci. USA 111 (49), 17,373–17,378.

Hong, Y.C., Pan, X.C., Kim, S.Y., Park, K., Park, E.J., Jin, X., Yi, S.M., Kim, Y.H., Park, C.H., Song, S., Kim, H., 2010. Asian Dust Storm and pulmonary function of school children in Seoul. Sci. Total Environ. 408 (4), 754–759.

Husar, R., et al., 2001. Asian dust events of April 1998. J. Geophys. Res. 106 (D16), 18,317–18,330.

In, H., Park, S., 2002. A simulation of long-range transport of yellow sand observed in April 1998 in Korea. Atmos. Environ. 36 (26), 4,173–4,187.

Korean Government, 2008. A Comprehensive Measure for Preventing the Damages of Yellow Dust. Ministry of Environment.

Korean Ministry of Environment, 2013. Comprehensive Measures to Reduce Particulate Matter. MOE.

Korean National Institute of Environmental Research, 2015. 2014 Annual Report of Ambient Air Quality in Korea. NIER.

Kwon, H.J., Cho, S.H., Chun, Y., Lagarde, F., Pershagen, G., 2002. Effects of the Asian dust events on daily mortality in Seoul, Korea. Environ. Res. 90 (1), 1–5.

Larson, E., 2014. China's Growing Coal Use Is World's Growing Problem. Climate Central. January 27. http://www.climatecentral.org/blogs/chinas-growing-coal-use-is-worlds-growing-problem-16999.

Lee, J., 2003. The Damages from Hwangsa and the Counterplan. Samsung Economic Research Institute. June 20. http://www.seri.org/db/dbReptV.html?g_menu=02&s_menu=0201&pubkey=db20031128001 (in Korean).

Leem, J.H., Kim, S.T., Kim, H.C., 2015. Public-health impact of outdoor air pollution for 2nd air pollution management policy in Seoul metropolitan area, Korea. Ann. Occup. Environ. Med. 27 (7).

Li, J., Yang, W., Wang, Z., Chen, H., Hu, B., Li, J., Sun, Y., Huang, Y., 2014. A modeling study of source-receptor relationships in atmospheric particulate matter over northeast Asia. Atmos. Environ. 91, 40–51.

Liu, T., He, G., Graff Zivin, J., 2018. Feel the Burn: Effects of Agricultural Straw Burning on Health in China. Working paper.

Liu, Z., Guan, D., Crawford-Brown, D., Zhang, Q., He, K., Liu, J., 2013. Energy policy: a low-carbon road map for China. Nature 500, 143–145.

Mori, I., Nishikawa, M., Tanimura, T., Quan, H., 2003. Change in size distribution and chemical composition of Kosa (asian dust) aerosol during long-range transport. Atmos. Environ. 37 (30), 4,253–4,263.

NASA, 2015. New NASA Satellite Maps Show Human Fingerprint on Global Air Quality. https://www.nasa.gov/press-release/new-nasa-satellite-maps-show-human-fingerprinton-global-air-quality.

Park, R., Han, G., 2014. Contribution of long-range transported air pollution from China to particulate matter over Korean peninsula. Magazine of KOSHAM 14 (2), 26–36.

Peters, G., Marland, G., Le Quere, C., Boden, T., Canadell, J., Raupach, M., 2012. Rapid growth in CO_2 emissions after the 2008-2009 global financial crisis. Nat. Clim. Chang. 2, 2–4.

Streets, D., Fu, J., Jang, C., Hao, J., He, K., Tang, X., Zhang, Y., Wang, Z., Li, Z., Zhang, Q., Wang, L., Wang, B., Yu, C., 2007. Air quality during the 2008 Beijing olympic games. Atmos. Environ. 41 (3), 480–492.

Uno, I., Amano, H., Emori, S., Kinoshita, K., Matsui, I., Sugimoto, N., 2001. Trans-pacific yellow sand transport observed in April 1998: a numerical simulation. J. Geophys. Res. 106 (D16), 18,331–18,344.

Zhang, D., 1984. Synoptic-climate studies of dust fall in China since the historic times. Sci. China, Ser. B 27 (8), 825–836.